Silapropargyl/Silaallenyl and Silylene Acetylide Complexes of [Cp(CO) 2 W] + . Theoretical Study of Their Interesting Bonding Nature and Formation Reaction

ARTICLE *in* JOURNAL OF THE AMERICAN CHEMICAL SOCIETY · OCTOBER 2006

Impact Factor: 12.11 · DOI: 10.1021/ja0625374 · Source: PubMed

5 AUTHORS, INCLUDING:

Mausumi Ray
Northwestern University
9 PUBLICATIONS **65** CITATIONS

SEE PROFILE

Yoshihide Nakao
Kyushu Sangyo University
78 PUBLICATIONS **1,583** CITATIONS

SEE PROFILE

J|A|C|S
ARTICLES
Published on Web 08/22/2006

Silapropargyl/Silaallenyl and Silylene Acetylide Complexes of $[Cp(CO)_2W]^+$. Theoretical Study of Their Interesting Bonding Nature and Formation Reaction

Mausumi Ray,[†] Yoshihide Nakao,[†] Hirofumi Sato,[†] Hiroyuki Sakaba,[§] and Shigeyoshi Sakaki*[,†,‡]

Contribution from the Department of Molecular Engineering, Graduate School of Engineering, Kyoto University, Kyotodaigaku-Katsura, Nishikyo-ku, Kyoto 615-8510, Japan, Fukui Institute for Fundamental Chemistry, Nishihiraki-cho, Takano, Kyoto 606-8103, Japan, and Department of Chemistry, Graduate School of Science, Tohoku University, Aoba-ku, Sendai 980-8578, Japan

Received April 21, 2006; E-mail: sakaki@moleng.kyoto-u.ac.jp

Abstract: The geometry and bonding nature of $Cp(CO)_2W(C{\equiv}CH)(SiH_2)$ (**1**) and the reaction leading to the formation of **1** from $Cp(CO)_2W(\overline{Si(H)_2C{\equiv}CH})$ (**9**) were theoretically investigated with DFT, MP2 to MP4(SDTQ), and CCSD(T) methods, where **9** and **1** were adopted as models of the interesting new complexes reported recently, $Cp^*(CO)_2W(\overline{Si(Ph)_2C{\equiv}C^tBu})$ and $Cp^*(CO)_2W(C{\equiv}C^tBu)(SiPh_2)$, respectively. Our computational results clearly indicate that **1** involves neither a pure silacyclopropenyl group nor pure silylene and acetylide groups and that the silylene group strongly interacts with both the W center and the acetylide group. Frontier orbitals of **1** resemble those observed in the formation of silacyclopropene from silylene and acetylene. The frontier orbitals, as well as the geometry, indicate that the $(CCH)(SiH_2)$ moiety of **1** can be understood in terms of an interesting intermediate species trapped by the W center in that formation reaction. Complex **1** is easily formed from **9** through Si−C σ-bond activation with moderate activation barriers of 15.3, 18.8, and 15.8 kcal/mol, which are the DFT-, MP4(SDTQ)-, and CCSD(T)-calculated values, respectively. This reaction takes place without a change of the oxidation state of the W center. Intermediate **9** is easily formed from $Cp(CO)_2W(Me)(H_3SiC{\equiv}CH)$ via Si−H oxidative addition, followed by C−H reductive elimination. The bonding nature of **9** is also very interesting; the nonbonding π-orbital of the H_2SiCCH moiety is essentially the same as that of the propargyl group, but the π-conjugation between Si and C atoms is very weak in the π-orbital, unlike that in the propargyl group.

Introduction

Transition metal−silylene complexes are important and interesting research targets in coordination chemistry, organometallic chemistry, and synthetic chemistry.[1−5] The geometry, bonding nature, and electronic structure are of considerable interest for comparison between transition metal−silylene complexes and their carbon analogues. The important role of these complexes as intermediates was also proposed in various metal-catalyzed transformation reactions of organosilicon compounds. To understand well their properties and reaction behavior, a considerable effort has been made to isolate transition metal−silylene complexes.[1−5] The first example of an isolated transition metal−silylene complex was reported by Schmidt and Welz in 1977.[6] However, $(CO)_4Fe(=SiMe_2NHEt_2)$, which they synthesized, was very unstable, and its X-ray characterization was not successful. In 1987, Zybill and Müller synthesized a transition metal−silylene complex and presented the first structural evidence for the TM=Si unit (TM = transition metal).[7] Since then, many successful results have been reported on the syntheses and characterization of transition metal−silylene complexes.[1−5] For instance, the Ogino group[8] and the Pannell group[9] successfully synthesized many transition metal−silylene complexes, from disilanyl complexes through a 1,2-silyl shift. The Tilley group successfully synthesized base-stabilized ruthenium−silylene complexes[10] and then base-free osmium− and platinum−silylene complexes.[11] The Corriu[12] and Braunstein groups[13] successfully synthesized HMPA- and amine-stabilized silylene complexes, respectively. The 1,2-H shift from a silyl ligand to a metal center was also employed to synthesize transition metal−silylene complexes.[14−16] It is noted

[†] Kyoto University.
[‡] Fukui Institute for Fundamental Chemistry.
[§] Tohoku University.

(1) Tilley, T. D. In *The Silicon−Heteroatom Bond*; Patai, S., Rappoprt, Z., Eds.; Wiley: New York, 1991; Chapters 9 and 10, pp 245, 309. (b) Eisen, M. S. In *The Chemistry of Organic Silicon Compounds*; Rappoport, Z., Apeloig, Y., Eds.; Wiley: New York, 1998; Vol. 2, Chapter 35, p 2037.
(2) Sharma, H. K.; Pannell, K. H. *Chem. Rev.* **1995**, *95*, 1351.
(3) (a) Braunstein, P.; Knorr, M. *J. Organomet. Chem.* **1995**, *500*, 21. (b) Braunstein, P.; Boag, N. M. *Angew. Chem., Int. Ed.* **2001**, *40*, 2427.
(4) (a) Ogino, H.; Tobita, H. *Adv. Organomet. Chem.* **1998**, *42*, 223. (b) Ogino, H. *Chem. Record* **2002**, *2*, 291. (c) Okazaki, M.; Tobita, H.; Ogino, H. *Dalton Trans.* **2003**, 493.
(5) Corey, J. Y.; Braddock-Wilking, J. *Chem. Rev.* **1999**, *99*, 175.
(6) Schmidt, G.; Welz, E. *Angew. Chem., Int. Ed. Engl.* **1977**, *16*, 785.
(7) Zybill, C.; Müller, G. *Angew. Chem., Int. Ed. Engl.* **1987**, *26*, 669.

Scheme 1

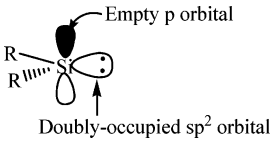

that σ-bond activation was involved as an important process in these syntheses of transition metal−silylene complexes. Besides these studies, transition metal−silylene complexes have also been synthesized by ligation of free silylene with the metal center.[17−21]

The transition metal−silylene complex has attracted considerable interest, as well.[22−26] The silylene species involves a singlet spin state, and as a result, the sp^2 lone-pair orbital and the empty p-orbital (Scheme 1) play important roles in the interaction with the metal center. This means that the coordinate bond with the transition-metal center is expected to be similar to that of CO. Unexpectedly, however, transition metal−silylene complexes are not stable, unlike transition metal−CO complexes. In this regard, the geometry and the bonding nature of transition metal−silylene complexes were theoretically discussed in many works.[22−25] The reaction of a transition metal−silylene complex is another attractive research subject for theoreticians. For instance, Hall and collaborators theoretically investigated the hydrosilation reaction catalyzed by a ruthenium−silylene complex.[26]

Recently, an interesting tungsten complex with composition $Cp^*(CO)_2W(C{\equiv}C^tBu)(SiPh_2)$ was synthesized from $Cp^*(CO)_2(MeCN)W(Me)$ and the alkynylsilane $(HPh_2SiC{\equiv}C^tBu)$,[27] as shown in Scheme 2. $Cp^*(CO)_2W(C{\equiv}C^tBu)(SiPh_2)$ is understood in terms of a tungsten−silylene complex stabilized by an intramolecular charge-transfer (CT) interaction with the acetylide group, as schematically shown by **Form-A** in Scheme 3, which is a new canonical structure of a transition metal−silylene complex. Two other renderings of this complex were also experimentally proposed: one is a tungsten complex involving a silacyclopropenyl group (**Form-B**), and the other is a tungsten complex with a four-membered ring including silyl and alkenyl groups (**Form-C**). It is worthwhile to investigate theoretically the bonding nature of $Cp^*(CO)_2W(C{\equiv}C^tBu)(SiPh_2)$ and to clarify which structure is correct. The formation of this compound is also very interesting, because this reaction takes place through a variety of σ-bond activation processes, as follows. In the experimentally proposed reaction scheme,[27] the first step is displacement of coordinated MeCN by the silylacetylene to give an intermediate $Cp^*(CO)_2W(Me)(HSi(Ph)_2C{\equiv}C^tBu)$ (**I-1**, Scheme 2), followed by Si−H oxidative addition to the W center to form the second intermediate, $Cp^*(CO)_2W(Me)(H)(Si(Ph)_2C{\equiv}C^tBu)$ (**I-2**). The next step is C−H reductive elimination of methane to form the third intermediate, $Cp^*(CO)_2W(\overline{Si(Ph)_2C{\equiv}C^tBu})$ (**I-3**), and the final step is either Si−C σ-bond activation to afford **Form-A** and **Form-C** or Si−C bond formation to afford **Form-B** (Scheme 3). If either **Form-A** or **Form-C** is correct, $Cp^*(CO)_2W(C{\equiv}C^tBu)(SiPh_2)$ is produced via a 1,2-alkynyl shift from a tungsten−1-alkynylsilyl complex, **I-3**, which, to our knowledge, is an interesting α-Si−C σ-bond activation.[28] Thus, it is worthwhile to investigate theoretically this formation reaction. Also, the bonding nature and geometry of **I-3** are interesting, because **I-3** is considered to be a silapropargyl complex, i.e., a silicon analogue of a propargyl complex; no such species has been reported yet, while the silicon analogue of a π-allyl complex has been experimentally reported.[29]

In the present study, the bonding nature of $Cp^*(CO)_2W(C{\equiv}C^tBu)(SiPh_2)$ and $Cp^*(CO)_2W(\overline{Si(Ph)_2C{\equiv}C^tBu})$ **I-3** and the reaction leading to the formation of $Cp^*(CO)_2W(C{\equiv}C^tBu)(SiPh_2)$ from $Cp^*(CO)_2W(Me)(HSi(Ph)_2C{\equiv}C^tBu)$ were theoretically investigated with DFT, MP2 to MP4(SDTQ), and CCSD(T) methods. The main purposes of this work are to present a proper understanding of the geometries and bonding nature of these complexes and to clarify electronic processes and characteristic features of the transformation from **I-1** to $Cp^*(CO)_2W(C{\equiv}C^tBu)(SiPh_2)$.

(8) (a) Tobita, H.; Ueno, K.; Ogino, H. *Chem. Lett.* **1986**, 1777. (b) Tobita, H.; Ueno, K.; Ogino, H. *Bull. Chem. Soc. Jpn.* **1988**, *61*, 2797. (c) Ueno, K.; Tobita, H.; Shimoi, M.; Ogino, H. *J. Am. Chem. Soc.* **1988**, *110*, 4092. (d) Tobita, H.; Ueno, K.; Shimoi, M.; Ogino, H. *J. Am. Chem. Soc.* **1990**, *112*, 3415. (e) Ueno, K.; Tobita, H.; Ogino, H. *Chem. Lett.* **1990**, 369. (f) Takeuti, T.; Tobita, H.; Ogino, H. *Organometallics* **1991**, *10*, 835. (g) Ueno, K.; Ito, S.; Endo, K.; Tobita, H.; Inomata, S.; Ogino, H. *Organometallics* **1994**, *13*, 3309. (h) Tobita, H.; Wada, H.; Ueno, K.; Ogino, H. *Organometallics* **1994**, *13*, 2545. (i) Ueno, K.; Nakano, K.; Ogino, H. *Chem. Lett.* **1996**, 459. (j) Ueno, K.; Masuko, A.; Ogino, H. *Organometallics* **1997**, *16*, 5026. (k) Okazaki, M.; Tobita, H.; Ogino, H. *Chem. Lett.* **1997**, 437. (l) Wada, H.; Tobita, H.; Ogino, H. *Chem. Lett.* **1998**, 993. (m) Ueno, K.; Sakai, M.; Ogino, H. *Organometallics* **1998**, *17*, 2138. (n) Ueno, K.; Masuko, A.; Ogino, H. *Organometallics* **1999**, *18*, 2694. (o) Tobita, H.; Sato, T.; Okazaki, M.; Ogino, H. *J. Organomet. Chem.* **2000**, *611*, 314. (p) Minglana, J. J. G.; Okazaki, M.; Tobita, H.; Ogino, H. *Chem. Lett.* **2002**, 406.
(9) (a) Pannell, K. H.; Cervantes, J.; Hernandez, C.; Cassias, J.; Vincenti, S. *Organometallics* **1986**, *5*, 1056. (b) Jones, K. L.; Pannell, K. H. *J. Am. Chem. Soc.* **1993**, *115*, 11336. (c) Jones, K. L.; Pannell, K. H. *Organometallics* **2001**, *20*, 7.
(10) Straus, D. A.; Tilley, T. D.; Rheingold, A. L.; Geib, J. S. *J. Am. Chem. Soc.* **1987**, *109*, 5872.
(11) (a) Grumbine, S. D.; Tilley, T. D.; Rheingold, A. L. *J. Am. Chem. Soc.* **1993**, *115*, 358. (b) Grumbine, S. D.; Tilley, T. D.; Arnold, F. P.; Rheingold, A. L. *J. Am. Chem. Soc.* **1993**, *115*, 7884.
(12) (a) Corriu, R. J. P.; Lanneau, G. F.; Chauhan, B. P. S. *Organometallics* **1993**, *12*, 2001. (b) Corriu, R. J. P.; Chauhan, B. P. S.; Lanneau, G. F. *Organometallics* **1995**, *14*, 1646. (c) Chauhan, B. P. S.; Corriu, R. J. P.; Lanneau, G. F.; Priou, C.; Auner, N.; Handwerker, H.; Herdtweck, E. *Organometallics* **1995**, *14*, 1657.
(13) Bodensieck, U.; Braunstein, P.; Dech, W.; Faure, T.; Knorr, M.; Stern, C. *Angew. Chem., Int. Ed. Engl.* **1994**, *33*, 2440.
(14) Chen, W.; Edwards, A. J.; Esteruelas, M. A.; Lahoz, F. J.; Olivan, M.; Oro, L. A. *Organometallics* **1996**, *15*, 2185.
(15) (a) Michell, G. P.; Tilley, T. D. *Angew. Chem., Int. Ed.* **1998**, *37*, 2524. (b) Michell, G. P.; Tilley, T. D. *J. Am. Chem. Soc.* **1998**, *120*, 7635. (c) Peters, J. C.; Feldman, J. D.; Tilley, T. D. *J. Am. Chem. Soc.* **1999**, *121*, 9871.
(16) Sakaba, H.; Tsukamoto, M.; Hirata, T.; Kabuto, C.; Horino, H. *J. Am. Chem. Soc.* **2000**, *122*, 11511.
(17) Denk, M.; Hayashi, R. K.; West, R. *J. Chem. Soc., Chem Commun.* **1994**, 33.
(18) Gehrhus, B.; Hitchcock, P. B.; Lappert, M. F.; Maciejewski, H. *Organometallics* **1998**, *17*, 5599.
(19) Petri, S. H. E.; Eikenberg, D.; Neumann, B.; Stammler, H. G.; Jutzi, P. *Organometallics* **1999**, *18*, 2615.
(20) Woo, L. K.; Smith, D. A.; Young, V. G., Jr. *Organometallics* **1991**, *10*, 3977.
(21) Feldman, J. D.; Mitchell, G. P.; Notle, J. O.; Tilley, T. D. *J. Am. Chem. Soc.* **1998**, *120*, 11184.
(22) Cundari, T. R.; Gordon, M. S. *J. Phys. Chem.* **1992**, *96*, 631.
(23) Marquez, A.; Sanz, J. F. *J. Am. Chem. Soc.* **1992**, *114*, 2903.
(24) Jacobsen, H.; Ziegler, T. *Organomettallics* **1995**, *14*, 224.
(25) Boheme, C.; Frenking, G. *Organometallics* **1998**, *17*, 5801.
(26) Beddie, C.; Hall, M. B. *J. Am. Chem. Soc.* **2004**, *126*, 13564.
(27) Sakaba, H.; Yoshida, M.; Kabuto, C.; Kabuto, K. *J. Am. Chem. Soc.* **2005**, *127*, 7276.
(28) (a) Burger, P.; Bergman, R. G. *J. Am. Chem. Soc.* **1993**, *115*, 10462. (b) Klei, S. R.; Tilley, T. D.; Bergman, R. G. *Organometallics* **2001**, *20*, 3220. (c) Klei, S. R.; Tilley, T. D.; Bergman, R. G. *Organometallics* **2002**, *21*, 4648. (d) Okazaki, M.; Suzuki, E.; Miyajima, N.; Tobita, H.; Ogino, H. *Organometallics* **2003**, *22*, 4633. (e) Suzuki, E.; Okazaki, M.; Tobita, H. *Chem. Lett.* **2005**, *34*, 1026.
(29) Sakaba, H.; Watanabe, S.; Kabuto, C.; Kabuto, K. *J. Am. Chem. Soc.* **2003**, *125*, 2842.

Scheme 2. Formation of $Cp^*(CO)_2W(C{\equiv}C^tBu)(SiPh_2)$ from $Cp^*(CO)_2W(Me)(MeCN)$

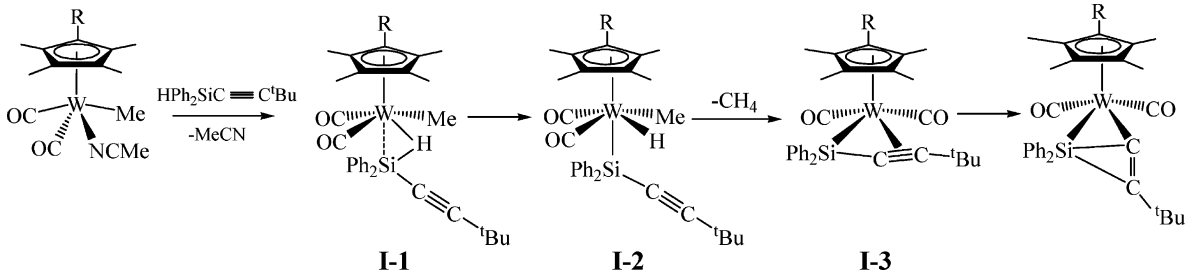

Scheme 3. Three Possible Limiting Forms of $Cp^*(CO)_2W(C{\equiv}C^tBu)(SiPh_2)$

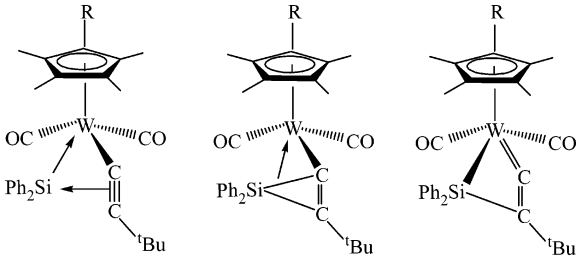

Computational Details

We employed here $Cp(CO)_2W(C{\equiv}CH)(SiH_2)$ (**1**) as the simplest model of $Cp^*(CO)_2W(C{\equiv}C^tBu)(SiPh_2)$. Geometries were optimized with the density functional theory (DFT) method, where the B3PW91 functional was adopted for the exchange-correlation terms.[30,31] The B3PW91 functional presented a much better agreement of the optimized geometry of **1** with the experimental one of $Cp^*(CO)_2W(C{\equiv}C^tBu)(SiPh_2)$[27] than the B3LYP[30,32] and MPWPW91[31,33] functionals (see Table S1, Supporting Information). We ascertained that none of the equilibrium geometries exhibited an imaginary frequency and each transition state exhibited only one imaginary frequency. Energy was evaluated with DFT, MP2 to MP4(SDTQ), and CCSD(T) methods, where the DFT-optimized geometries were adopted.

Two kinds of basis set systems, BS-I and BS-II, were used in this work. In BS-I, the usual LANL2DZ[34] basis set was employed for W. The cc-pVDZ basis set[35] was employed for Si, C, and O, and the 6-31G basis set was used for H.[36] This BS-I system was used for geometry optimization. The basis set effects on the optimized geometry were examined with the 6-31G(d)[37] basis set for Si, C, and O and the Huzinaga−Dunning[38] basis set for Si. However, no significant difference was observed between BS-I and these basis set systems (see Table S1). In BS-II, the valence electrons of W were represented with a (541/541/111/1) basis set[34,39,40] with the same effective core potentials as those of BS-I. For the other atoms, the same basis sets as those of BS-I were employed. This BS-II was used to evaluate energy and population changes.

The Gaussian 03 program package (revision C.02)[41] was used for all these computations. Population analysis was carried out with the method proposed by Weinhold et al.[42] Molecular orbitals were drawn with the MOLEKEL program package (version 4.3).[43]

Results and Discussion

In this article, we discuss first the bonding nature and geometry of $Cp^*(CO)_2W(C{\equiv}C^tBu)(SiPh_2)$ and then the reaction leading to its formation from $Cp^*(CO)_2W(Me)(Si(Ph)_2HC{\equiv}C^tBu)$. Also, we discuss the bonding nature and characterization of $Cp^*(CO)_2W(\overline{Si(Ph)_2C{\equiv}C^tBu})$ in comparison with those of similar propargyl/allenyl complexes.

Geometry of $Cp(CO)_2W(C{\equiv}CR^1)(SiR^2_2)$ (R^1 = H, Me, or ^{t}Bu; R^2 = H or Me). The optimized geometry of $Cp(CO)_2W(C{\equiv}CH)(SiH_2)$ (**1**) agrees well with the experimental one,[27] except for a few geometrical parameters: the W−Si and Si−C1 distances are moderately longer but the W−C1 and Si−C2 distances are moderately shorter than the corresponding experimental values (see Figure 1 and Table 1 for important geometrical parameters). Introduction of Me and ^{t}Bu groups on the acetylide C atom leads to excellent agreement of the optimized geometry with the experimental one, as will be discussed below in more detail.

For a better understanding of the geometry and bonding nature of **1**, we optimized an ideal complex, $Cp(CO)_2W(C{\equiv}CH)(SiH_2)$ (**2**), in which the acetylide group is at a position opposite to the SiH_2 group, as shown in Figure 1; in other words, no interaction exists between these two moieties. The W−C1 and C1−C2 distances of **2** agree well with those of a typical tungsten−acetylide complex.[44] Silacyclopropene **3** was also optimized, as shown in Figure 2. The Si−C and C−C distances of **3** agree well with the experimental values.[45]

The Si−C1 and Si−C2 distances in **1** are considerably longer than the Si−C bond of **3**. Consistent with these long Si−C1 and Si−C2 distances, the C1−C2 distance of **1** is somewhat shorter than that of **3**. Also, the C1−C2 distance is longer in **1**

(30) (a) Becke, A. D. *Phys Rev. A.* **1988**, *38*, 3098. (b) Becke, A. D. *J. Chem. Phys.* **1993**, *98*, 5648.
(31) (a) Perdew, J. P. In *Electronic Structure of Solids '91*; Ziesche, P., Eschrig, H., Ed.; Akademic Verlag: Berlin, 1991; p 11. (b) Perdew, J. P.; Chevary, J. A.; Vosko, S. H.; Jackson, K. A.; Pederson, M. R.; Singh, D. J.; Fiolhais, C. *Phys. Rev. B* **1992**, *46*, 6671. (c) Perdew, J. P.; Chevary, J. A.; Vosko, S. H.; Jackson, K. A.; Pederson, M. R.; Singh, D. J.; Fiolhais, C. *Phys. Rev. B* **1993**, *48*, 4978. (d) Perdew, J. P.; Burke, K.; Wang, Y. *Phys. Rev. B* **1996**, *54*, 16533.
(32) Lee, C.; Yang, W.; Parr, R. G. *Phys. Rev. B* **1988**, *37*, 785.
(33) Adamo, C.; Barone, V. *J. Chem. Phys*. **1998**, *108*, 664.
(34) Hay, P. J.; Wadt, W. R. *J. Chem. Phys*. **1985**, *82*, 299.
(35) (a) Dunning, T. H., Jr. *J. Chem. Phys*. **1989**, *90*, 1007. (b) Woon, D. E.; Dunnin, T. H.g, Jr. *J. Chem. Phys*. **1993**, *98*, 1358.
(36) Ditchfield, R.; Hehre, W. J.; Pople, J. A. *J. Chem. Phys.* **1971**, *54*, 724.
(37) (a) Hehre, W. J.; Ditchfield, R.; Pople, J. A. *J. Chem. Phys*. **1972**, *56*, 2257. (b) Hariharan, P. C.; Pople, J. A. *Theor. Chim. Acta* **1973**, *28*, 213. (c) Francl, M. M.; Petro, W. J.; Hehre, W. J.; Binkley, J. S.; Gordon, M. S.; Defrees, D. J.; Pople, J. A. *J. Chem. Phys* **1982**, *77*, 3654.
(38) Dunning, T. H., Jr. In *Modern Theoretical Chemistry, Vol. 3*; Schaefer, H. F., III, Ed.; Plenum: New York, 1976; pp 1−28. The d polarization function (ζ = 0.3247) implemented in the Gaussian 03 program package (revision C.02) was used for Si.
(39) Couty, M.; Hall, M. B. *J. Comput. Chem*. **1996**, *17*, 1359.
(40) Ehlers, A. W.; Bohme, D. S.; Gobbi, A.; Hollwarth, A.; Jonas, V.; Kohler, K. F.; Stegmann, R.; Veldkamp, A.; Frenking, G. *Chem. Phys. Lett*. **1993**, *208*, 111.
(41) Pople, J. A.; et al. *Gaussian 03*, Revision C.02; Gaussian Inc.: Wallingford, CT, 2004.
(42) Glendening, E. D.; Reed, A. E.; Carpenter, J. E.; Weinhold, F. NBO, Version, 3.1.
(43) (a) Flükiger, P.; Lüthi, H. P.; Portmann, S.; Weber, J. *MOLEKEL 4.3*; Swiss Center for Scientific Computing: Manno, Switzerland, 2000−2002. (b) Portmann, S.; Lüthi, H. P. *MOLEKEL*, An Interactive Molecular Graphics Tool. *CHIMIA* **2000**, *54*, 766−770.
(44) Pin, C.-W.; Peng, J.-J.; Shiu, C.-W.; Chi, Y.; Peng, S.-M.; Lee, G.-H. *Organometallics* **1998**, *17*, 438.
(45) Tutsui, S.; Sakamoto, K.; Kabuto, C.; Kira, M. *Organometallics* **1998**, *17*, 3819.

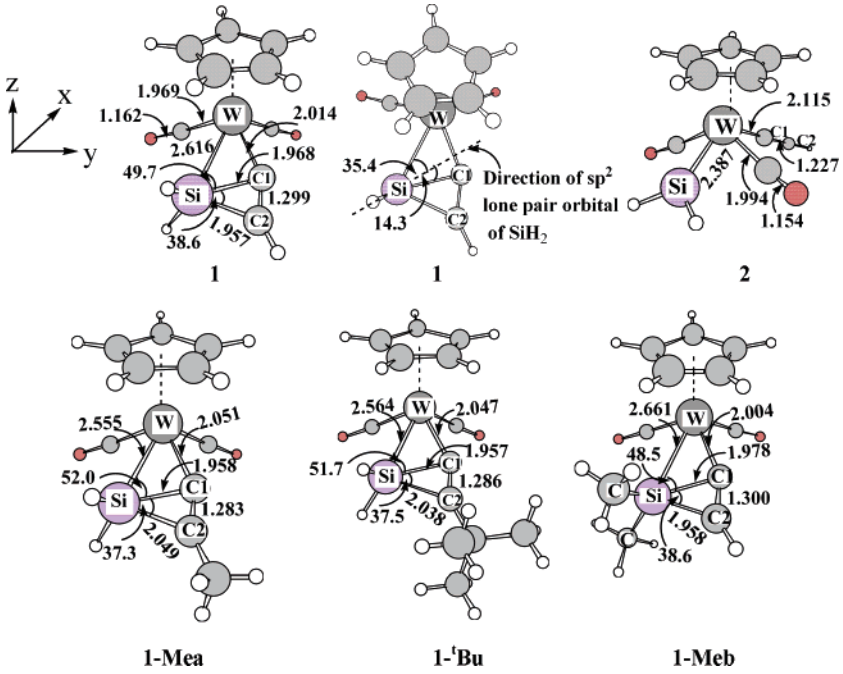

Figure 1. DFT/BS-I-optimized geometries[a] of $Cp(CO)_2W(C{\equiv}CR^1)(SiR^2_2)$ (R^1 = H, Me, or ^{t}Bu; R^2 = H or Me). [a]Bond lengths are in angstroms, and bond angles are in degrees.

Table 1. Selected Optimized Parameters of $Cp(CO)_2W(C{\equiv}CR^1)(SiR^2_2)$[a]

	1, R^1 = H, R^2 = H	**1-Mea**, R^1 = Me, R^2 = H	**1-^{t}Bu**, R^1 = ^{t}Bu, R^2 = H	**1-Meb**, R^1 = H, R^2 = Me	expt,[b] R^1 = ^{t}Bu, R^2 = Ph
W−Si	2.616	2.555	2.564	2.661	2.567
W−C1	2.014	2.051	2.047	2.004	2.050
Si−C1	1.968	1.958	1.957	1.978	1.937
Si−C2	1.957	2.049	2.038	1.958	2.009
C1−C2	1.299	1.283	1.286	1.300	1.270
∠W−Si−C1	49.7	52.0	51.7	48.5	51.9
∠C1−Si−C2	39.0	37.3	37.5	38.6	37.5

[a] Bond lengths are in angstroms, and bond angles are in degrees. [b] Reference 27.

than in **2**. It is noted that the acetylide moiety is somewhat distorted in **1** (C1−C2−H angle = 145.7°), unlike the linear alignment in **2**. The W−C1 distance of **1** is almost the same as that of **2**, while the W−Si distance of **1** is longer than those of **2** and a typical donor-stabilized tungsten−silylene complex.[8m,46] Consistent with the longer W−Si distance in **1** than in **2** and the longer Si−C1 and Si−C2 distances in **1** than in **3**, the sp^2 lone-pair orbital of SiH_2 expands neither toward the W center nor toward the midpoint of the C1−C2 bond; i.e., the sp^2 lone-pair orbital expands at an angle of 35° with the W−Si bond and at an angle of 14° with the Si−C1 bond, as shown in Figure 1.

All these geometrical features of **1** suggest that the CCH-(SiH_2) moiety in **1** is neither a pure silacyclopropenyl group nor the sum of pure silylene and acetylide groups. It is likely that the CCH(SiH_2) moiety is intermediate between them, which will be discussed below in more detail.

To shed light on the CCH(SiH_2) moiety, we investigated the formation of silacyclopropene from silylene and acetylene, as shown in Figure 2. This reaction takes place without barrier, as previously reported by Gordon et al.[47] and Koch et al.[48] Because no precursor complex could be optimized in this reaction, the starting geometry $\mathbf{4}_{-1}$ was optimized under the assumption that the SiH_2 plane was parallel to the C−C bond. In $\mathbf{4}_{-1}$, the Si−C distances are long and the sp^2 lone-pair orbital of SiH_2 makes a large angle (72.9°) with the Si−C bond. Upon going to $\mathbf{4}_{-3}$ from $\mathbf{4}_{-1}$, the sp^2 lone-pair orbital of SiH_2 is changing its direction toward the center of the C−C bond, with concomitant formation of two Si−C bonds. The angle (14.3°) between the sp^2 lone-pair orbital and the Si−C1 bond in **1** is smaller than that (26.3°) of $\mathbf{4}_{-2}$ but larger than that (1.1°) of $\mathbf{4}_{-3}$. The Si−C1 and Si−C2 distances of **1** are not very much different from those of $\mathbf{4}_{-2}$. From these geometrical features, it is concluded that the CCH(SiH_2) moiety of **1** is similar to the HCCH(SiH_2) species halfway to the formation of silacyclopropene from silylene and acetylene; in other words, the CCH(SiH_2) moiety of **1** is understood to be an interesting intermediate species trapped by the W center in the reaction leading to the formation of silacyclopropene.

Substituent effects on the geometry of **1** were investigated by introducing Me and ^{t}Bu on C2 and Me on Si (see **1-Mea**, **1-^{t}Bu**, and **1-Meb** in Figure 1). Introduction of Me and ^{t}Bu groups on C2 considerably shortens the W−Si distance by 0.061 and 0.052 Å, respectively, and considerably lengthens the Si−C2 distance by 0.092 and 0.081 Å, respectively (see **1-Mea** and **1-^{t}Bu** in Figure 1). The C1−C2 bond also becomes moderately shorter upon introduction of Me and ^{t}Bu groups on C2. Consistent with the shortening of the W−Si distance, the angle between the sp^2 lone-pair orbital of SiH_2 and the W−Si bond decreases to 25.4° in **1-Mea** and 27.4° in **1-^{t}Bu**, compared to 35.4° in **1**. These optimized geometries of **1-Mea** and **1-^{t}Bu** extremely agree with the experimental one. On the other hand, the presence of Me groups on Si little changes the geometry, except for moderate lengthening of the W−Si distance in

(46) Sakaba, H.; Tsukamoto, M.; Hirata, T.; Kabuto, C.; Horino, H. *J. Am. Chem. Soc.* **2000**, *122*, 11511.
(47) Chung, G.; Gordon, M. S. *Organometallics* **1999**, *18*, 4881.
(48) Koch, R.; Bruhn, T.; Weidenbruch, M. *Organometallics* **2004**, *23*, 1570.

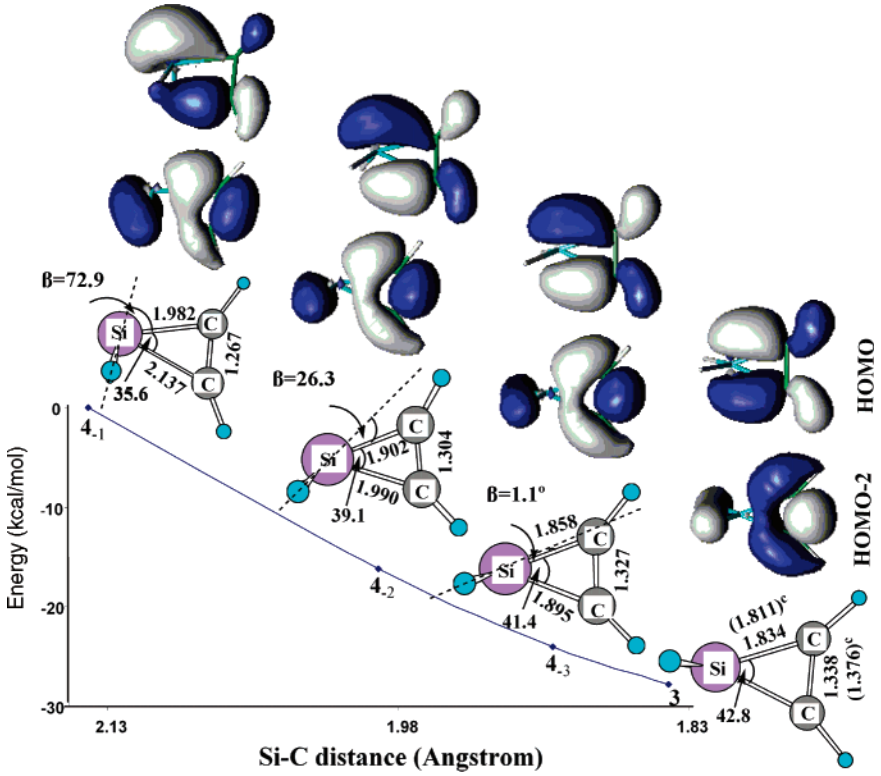

Figure 2. Changes of geometry,[a] total energy,[b] and important Kohn−Sham orbitals[b] in the formation of silacyclopropene from silylene and acetylene. [a]DFT/ BS-I optimization was carried out. Bond lengths are in angstroms, and bond angles are in degrees. [b]DFT/BS-II calculation. [c]In parentheses are experimental values.[45]

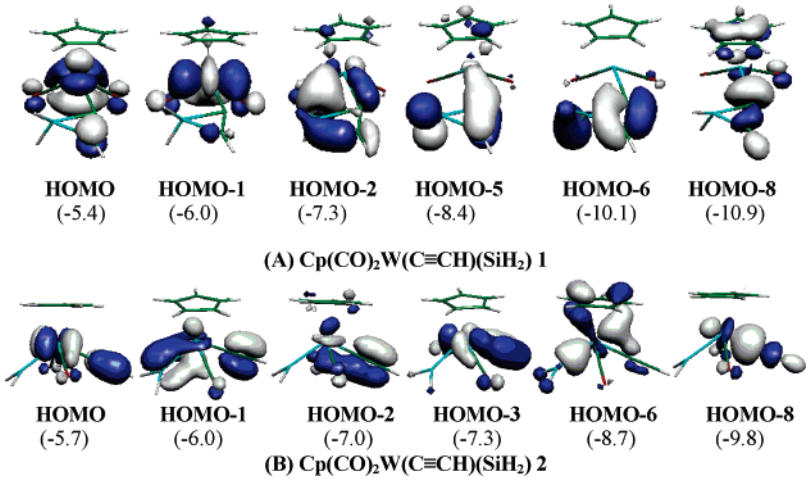

Figure 3. Several important Kohn−Sham orbitals observed in $Cp(CO)_2W(C{\equiv}CH)(SiH_2)$ (**1**) and ideal complex $Cp(CO)_2W(C{\equiv}CH)(SiH_2)$ (**2**). In parentheses are orbital energies (in eV).

1-Meb. These substituent effects will be discussed below on the basis of the bonding nature.

Bonding Nature of $Cp(CO)_2W(C{\equiv}CH)(SiH_2)$ (1). To clearly understand the bonding nature of **1**, we investigated the molecular orbitals of **1**. The HOMO and HOMO-1 mainly consist of a W d-orbital, as shown in Figure 3A. The presence of two doubly occupied d-orbitals is consistent with the 2+ oxidation state of W (d^4 system). The HOMO-2 of **1** closely resembles the HOMO of silacyclopropene, and the HOMO-6 of **1** is similar to the HOMO-2 of $\mathbf{4}_{-1} \sim \mathbf{4}_{-3}$ (see also Figure 2). These features suggest that the HOMO-2 and HOMO-6 of **1** mainly consist of the sp^2 lone-pair and empty p-orbitals of silylene and the π- and π*-orbitals of acetylide. The sp^2 lone-pair orbital of silylene overlaps with the π*-orbital of acetylide in a bonding way, because the π*-orbital is at higher energy than the sp^2 lone-pair orbital, and with the π-orbital of acetylide in an antibonding way, because the π-orbital is at lower energy than the sp^2 lone-pair orbital, as shown in Scheme 4A. As a result, the contribution of the C1 p-orbital considerably decreases and that of the C2 p-orbital considerably increases, which leads to the HOMO-2. In other words, the HOMO-2 involves CT from the sp^2 lone pair of silylene to the π*-orbital of acetylide and a four-electron repulsion between the sp^2 lone pair of silylene and the π-orbital of acetylide. The HOMO-6 is formed through slightly different orbital mixing: the π-orbital of acetylide overlaps with the sp^2 lone-pair orbital of silylene in a bonding way because the HOMO-6 is the most stable in energy among the molecular orbitals consisting of the π- and π*-orbitals of

Scheme 4

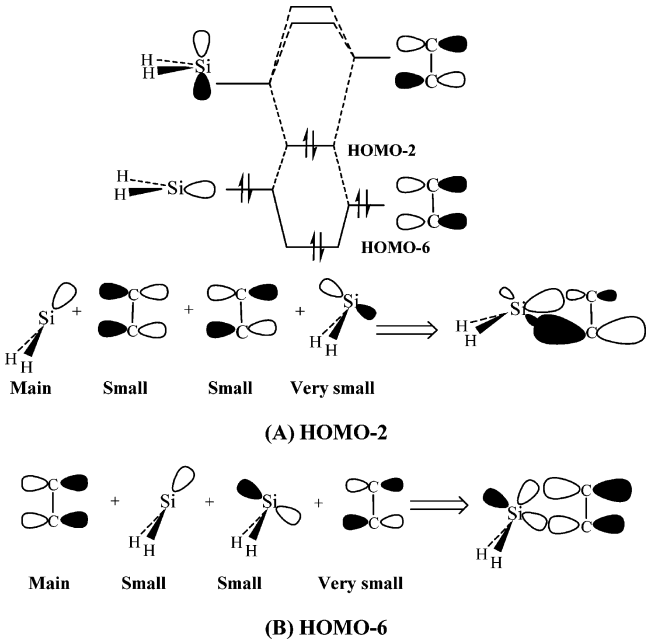

Table 2. π- and π*-Orbital Energies of Acetylene and sp^2 Lone-Pair and Empty p-Orbital Energies of Silylene

$[H-C\equiv C-R^1]^b$			
	orbital energy[a] (eV)		
orbital	$R^1 = H$	$R^1 = Me$	$R^1 = {}^tBu$
π	−7.78 (−10.6)	−7.15 (−9.99)	−7.02 (−9.85)
π*	−0.67 (3.57)	0.14 (4.38)	0.09 (4.31)

$SiR^2{}_2{}^c$		
	orbital energy[a] (eV)	
orbital	$R^2 = H$	$R^2 = Me$
sp^2 lone pair	−6.01 (−8.47)	−5.19 (−7.68)
p	−3.28 (0.26)	−2.19 (1.29)

[a] The DFT/BS-II calculation. In parentheses are Hartree−Fock orbital energies (BS-II). [b] Orbitals of free $HCCR^1$ are presented, where the geometry was taken to be the same as that in $Cp(CO)_2W(C\equiv CR^1)(SiR^2{}_2)$ (R^1 = H, Me, or ^{t}Bu; R^2 = H or Me) (see Figure S1, Supporting Information). [c] Orbitals of free silylene are presented. Geometries are optimized with the DFT/BS-I method.

acetylide and the sp^2- and p-orbitals of silylene. Into this overlap, the empty p-orbital of silylene mixes in a bonding way with the π-orbital of acetylide because the empty p-orbital is at higher energy than the π-orbital. The π*-orbital of acetylide also slightly mixes into this orbital in a bonding way with the sp^2 lone-pair orbital of silylene. These orbital mixings lead to bonding overlap of the deformed π-orbital of acetylide with the empty p- and sp^2 lone-pair orbitals of silylene, as shown in Scheme 4B. In other words, the HOMO-6 involves CT from the π-orbital of acetylide to the empty p-orbital of silylene.

Comparison of **1** with **2** provides us information of the W−Si and W−C1 bonding nature of **1**. In **2**, the SiH_2 moiety is bound to the W center through donation from the sp^2 lone-pair orbital to the empty d-orbital of W, which is observed in the HOMO-6 of **2**, as shown in Figure 3B. In **1**, on the other hand, there is no clear bonding overlap, but a deformed bonding overlap between W and Si centers is observed in the HOMO-2, as shown in Figure 3A. This deformed overlap can be easily understood in terms of the bonding orbital between the sp^2 lone-pair orbital of silylene and the π*-orbital of acetylide (Scheme 4A) interacting with the empty d-orbital of W. Although silacyclopropene is formed from silylene and acetylene in the absence of $Cp(CO)_2W$, SiH_2 cannot completely change its orientation toward the C1−C2 bond in the presence of $Cp(CO)_2W$. This is because the bonding overlap between the sp^2 lone pair of SiH_2 and the empty d-orbital of W suppresses the complete change of the SiH_2 orientation. Also, the occupied d_{z^2}-orbital overlaps well with the empty p-orbital of SiH_2 in **2**, to allow the d_π−p back-donating interaction, which is observed in the HOMO-1 of **2**. However, the d_{z^2}-orbital does not form such an interaction in **1**, as shown by the HOMO of **1**. These results indicate that **1** does not involve a pure silylene group, unlike **2**, which is consistent with the discussion based on the geometrical features. In **2**, the HOMO-3 involves the bonding overlap between the π-orbital of acetylide and the unoccupied d_{xy}-orbital of W (Figure 3). Its antibonding counterpart is the HOMO. Similar orbitals are observed in the HOMO-5 and the HOMO of **1**, respectively. The HOMO-8 of **1** and **2** involves a bonding interaction between the unoccupied d_{xz}-orbital of W and the sp lone pair of acetylide. These results suggest that the interaction between acetylide and W in **1** is similar to that of the normal acetylide ligand, which is consistent with the similar W−C1 distances in **1** and **2**.

From all these results, it can be clearly concluded that the $CCH(SiH_2)$ moiety of **1** is neither a pure silacyclopropenyl group nor the sum of pure silylene and acetylide groups. In **1**, the acetylide group strongly interacts with silylene through the CT from the π-orbital of acetylide to the empty p-orbital of silylene and the CT from the sp^2 lone pair of silylene to the π*-orbital of acetylide. Despite these strong CT interactions, the $CCH(SiH_2)$ moiety does not change to a pure silacyclopropenyl group because of the bonding interaction between the sp^2 lone-pair orbital of silylene and the empty d-orbital of W. Thus, the $CCH(SiH_2)$ moiety of **1** is understood to be an interesting intermediate species which is trapped by the W center in the reaction leading to the formation of silacyclopropene from acetylene and silylene.

Substituent Effects on the Bonding Nature of $Cp(CO)_2W(C\equiv CR^1)(SiR^2{}_2)$. Significant substituent effects on the Si−C and W−Si distances were observed when Me and ^{t}Bu groups were introduced on the C2 atom, as described above. These substituent effects are interpreted in terms of the π- and π*-orbitals of the acetylide group. Their orbital energy becomes higher upon introduction of electron-donating substituents, as shown in Table 2. Both the bonding interaction of the acetylide π-orbital with the silylene empty p-orbital and the antibonding interaction of the acetylide π-orbital with the silylene sp^2 lone-pair orbitals become stronger as the π-orbital of acetylide increases in energy. Considering that the introduction of Me and ^{t}Bu groups on C2 increases the Si−C2 distance, it is concluded that the antibonding interaction is greater than the bonding interaction. In other words, the repulsive interaction between the sp^2 lone-pair orbital of silylene and the π-orbital of acetylide is still strong in **1**. This repulsive interaction shifts the direction of the lone-pair orbital of silylene toward the W center from the C1 atom in **1-Mea** and **1-^{t}Bu**. As a result, the electron-donating substituent on C2 strengthens the coordinate

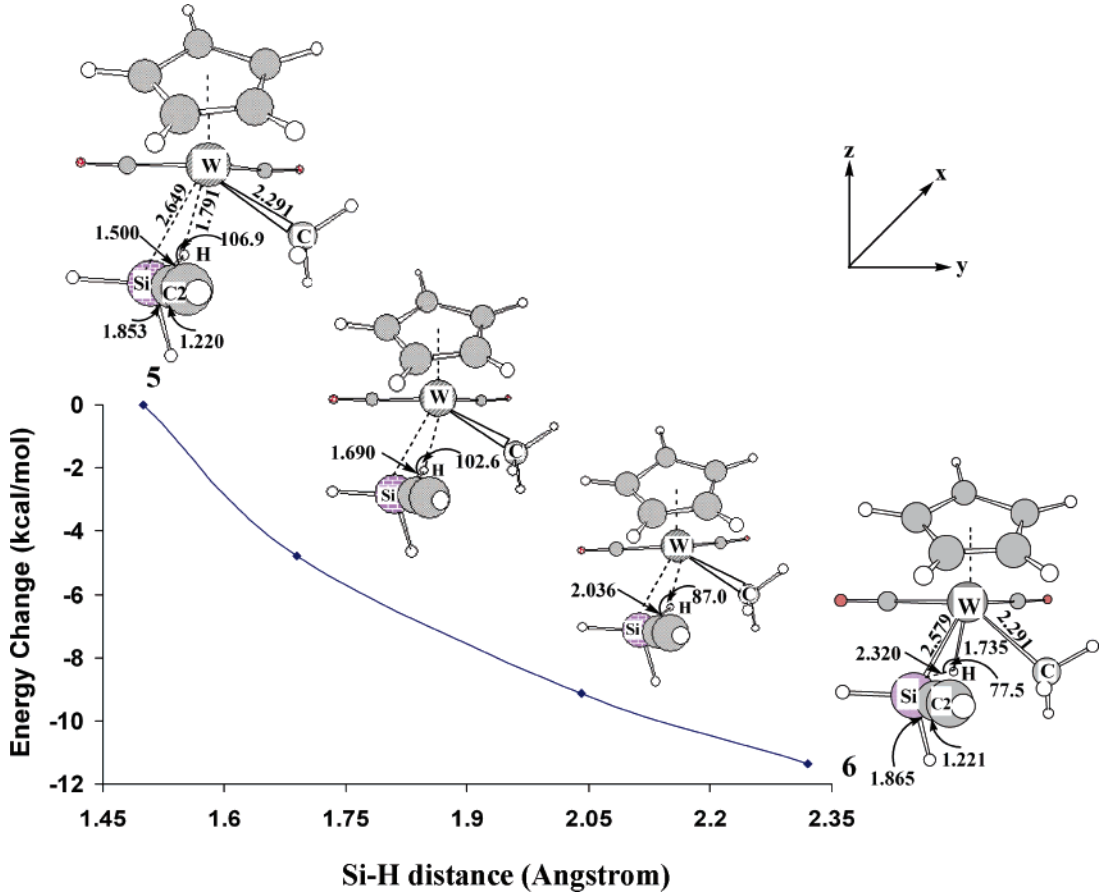

Figure 4. Geometry[a] and energy[b] changes resulting from the conversion of $Cp(CO)_2W(CH_3)(H_3SiC{\equiv}CH)$ (**5**) to $Cp(CO)_2W(CH_3)(H)(H_2SiC{\equiv}CH)$ (**6**). [a]DFT/BS-I optimization was carried out. Bond lengths are in angstroms, and bond angles are in degrees. [b]DFT/BS-II calculation (in kcal/mol).

bond of silylene with the W center, which shortens the W−Si distance in **1-Mea** and **1-^{t}Bu** compared to that in **1**.

Introduction of Me on Si raises the energy of the sp^2 lone-pair orbital and the empty p-orbital of the silylene (Table 2). As the sp^2 lone-pair orbital becomes higher in energy, both the bonding and antibonding interactions of the sp^2 lone pair of silylene with the π*- and π-orbitals of acetylide, respectively, become stronger. However, the bonding interaction between the empty p-orbital of silylene and the π-orbital of acetylide becomes weaker. Because these effects compensate each other, the Si−C1, Si−C2, and W−C1 distances change little in **1-Meb**. However, the W−Si distance becomes moderately longer in **1-Meb** than in **1**. This is interpreted as follows: The electron-donating group on Si decreases the participation of the empty p-orbital in the bonding interaction with the π-orbital of acetylide but increases the participation of the sp^2 lone pair in the bonding interaction with the π*-orbital of acetylide. As a result, the direction of the lone-pair orbital of SiH_2 shifts toward C1, which weakens the W−Si interaction and thereby increases the W−Si distance.

Conversion from $Cp(CO)_2W(Me)(SiH_3C{\equiv}CH)$ to $Cp(CO)_2W(\overline{Si(H)_2C{\equiv}CH})$. We wished to investigate the reaction from $Cp(CO)_2W(Me)(SiH_3C{\equiv}CH)$ (**5**) to $Cp(CO)_2W(\overline{Si(H)_2C{\equiv}CH})$ because interesting elementary steps and intermediates are involved. This conversion takes place through two steps. In the first step, **5** converts to $Cp(CO)_2W(Me)(H)(Si(H)_2C{\equiv}CH)$ (**6**) through Si−H oxidative addition. In the second step, **6** converts to $Cp(CO)_2W(Si(H)_2C{\equiv}CH)(CH_4)$ (**7**) through reductive elimination of methane.

The conversion of **5** to **6** takes place without any barrier, as shown in Figure 4. Geometry optimization of **5** smoothly leads to **6**, where the geometry of **5** was optimized with the Si−H distance fixed to be the same as that of the free $HCCSiH_3$ molecule. The Si−H bond gradually lengthens and the W−Si and W−H distances gradually shorten upon going to **6** from **5**. In **6**, the Si−H distance is 2.320 Å, and the W−H and W−Si distances are 1.735 and 2.579 Å, respectively. These geometrical features indicate that the Si−H σ-bond is completely broken and the W−Si and the W−H bonds are formed in **6**. This conversion reaction is considerably exothermic, as shown in Table 3. Though the DFT-calculated reaction energy (ΔE) is moderately different from the MP4(SDTQ)-calculated value, the ΔE value fluctuates little upon going to MP4(SDTQ) from MP2, suggesting that the MP4(SDTQ) value is reliable.

To understand this conversion reaction, we examined several important molecular orbitals. In **5**, HOMO and HOMO-1 mainly consist of a d-orbital, while the other three d-orbitals are involved in unoccupied space (see Figure S2A, Supporting Information). These results indicate that the W center takes a 2+ oxidation state in **5**. In **6**, it is noted that only one d-orbital of W is in occupied space and the remaining four d-orbitals are in unoccupied space, which clearly shows that the doubly occupied d_{z^2}-orbital becomes unoccupied and the W center takes a 4+ oxidation state in **6** (see Figure 4 for the coordinate system). The HOMO-4 involves the bonding overlap between

Table 3. Activation Barrier (E_a), Reaction Energy (ΔE), and Destabilization Energy (DE) in the Conversion Reactions from $Cp(CO)_2W(Me)(H_3SiC{\equiv}CH)$ (**5**) to $Cp(CO)_2W(Me)(H)(Si(H)_2C{\equiv}CH)$ (**6**), from **6** to $Cp(CO)_2W(CH_4)(Si(H)_2C{\equiv}CH)$ (**7**), and from $Cp(CO)_2W(Si(H)_2C{\equiv}CH)$ (**8**) to $Cp(CO)_2W(Si(H)_2C{\equiv}CH)$ (**9**)[a]

	conversion of **5** to **6**	conversion of **6** to **7**		methane dissociation from **7** (**7** → **8**)	conversion of **8** to **9**
method	ΔE (kcal/mol)	E_a (kcal/mol)	ΔE (kcal/mol)	DE (kcal/mol)	ΔE (kcal/mol)
DFT	−11.4	10.7	−0.6	8.2	−31.2
MP2	−13.0	10.0	2.9	18.4	−45.8
MP3	−14.7	16.0	2.6	10.2	−26.6
MP4(DQ)	−15.4	14.4	3.9	13.4	−34.9
MP4(SDQ)	−15.5	14.8	3.7	13.9	−34.5
MP4(SDTQ)	−14.2	11.8	2.6	17.5	−43.3

[a] E_a is the energy difference between transition state and reactant, ΔE is the energy difference between product and reactant, and DE is the destabilization energy induced by methane dissociation. BS-II was employed.

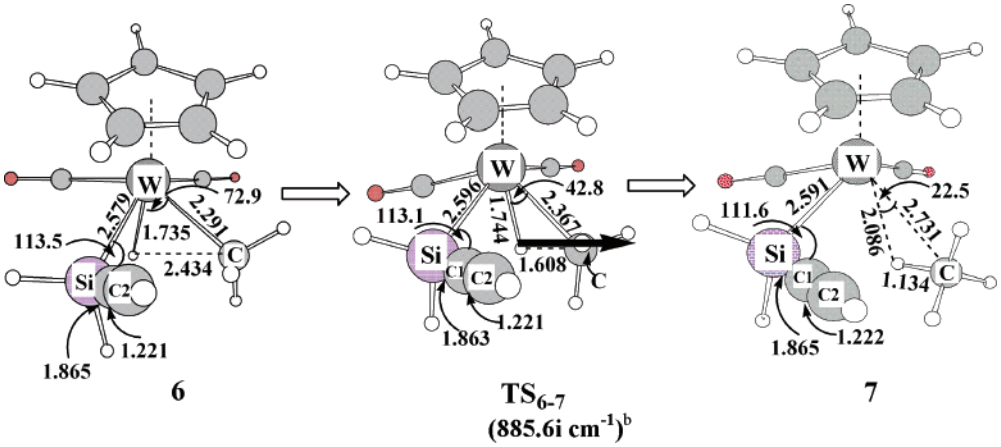

Figure 5. Geometry changes[a] resulting from the reductive elimination of methane from $Cp(CO)_2W(Me)(H)(Si(H)_2C{\equiv}CH)$ (**6**) to afford $Cp(CO)_2W(CH_4)(Si(H)_2C{\equiv}CH)$ (**7**). [a]DFT/BS-I optimization was carried out. Bond lengths are in angstroms, and bond angles are in degrees. [b]Arrow in $\mathbf{TS_{6-7}}$ represents important movement of atom in imaginary frequency. Imaginary frequency is given in parentheses. DFT/BS-I calculation.

the 1s-orbital of H and the empty d_{z^2}-orbital of W, and the HOMO-1 involves the bonding overlap between the sp^3 lone pair of Si and the empty d-orbital of W (see Figure S2B). All these results are consistent with our understanding that the Si−H oxidative addition takes place in this process.

The intermediate **6** converts to $Cp(CO)_2W(Si(H)_2C{\equiv}CH)(CH_4)$ (**7**) through transition state $\mathbf{TS_{6-7}}$, as shown in Figure 5. In $\mathbf{TS_{6-7}}$, there is only one imaginary frequency (885.6i cm^{-1}), involving the movement of the hydride ligand toward the Me ligand. In this transition state, the W−C distance lengthens moderately (by 0.076 Å) to 2.367 Å, and the W−H distance becomes slightly longer. The C−H distance is still long. These geometrical features indicate that the W−H and W−C bonds are maintained and the C−H bond is not yet effectively formed in $\mathbf{TS_{6-7}}$; in other words, this transition state is reactant-like. In **7**, the C−H distance is 1.134 Å, which clearly shows that methane is completely formed in **7** and interacts with the W center through a weak interaction, similar to the agostic interaction because its C−H distance is somewhat longer than the usual C−H bond. This reaction takes place easily with moderate activation barrier and either very small exothermicity (DFT/BS-II) or small endothermicity (MP4(SDTQ)/BS-II) (see Table 3); the activation barrier somewhat fluctuates at MP3 but converges upon going to MP4(SDTQ) from MP2. Also, the MP4(SDTQ)-calculated value is almost the same as the DFT-calculated value. The moderate activation barrier is consistent with the reactant-like $\mathbf{TS_{6-7}}$. Though the reaction energy is slightly different between DFT and MP4(SDTQ) methods, the difference is not large, indicating that this reaction is almost thermoneutral. The orbital changes observed in this reductive elimination are the reverse of those observed in the oxidative addition of the Si−H bond. We omitted detailed discussion here; see Figure S2 in the Supporting Information for orbital changes in this reductive elimination and the corresponding discussion.

Methane dissociation from **7** leads to a coordinatively unsaturated complex, $Cp(CO)_2W(Si(H)_2C{\equiv}CH)$ (**8**), with moderate destabilization energy, where the geometry of **8** was taken to be the same as that of **7**, except for the absence of a methane moiety. The destabilization energy (DE) is evaluated to be 8.2 and 17.5 kcal/mol with the DFT and MP4(SDTQ) methods, respectively (Table 3). Because the DFT method does not incorporate well the dispersion interaction, which participates considerably in the interaction of methane with the metal center, the MP4(SDTQ)-calculated value is more reliable here than the DFT-calculated value. In **8**, the C≡C triple bond does not interact with the W center. The geometry optimization of **8** smoothly leads to $Cp(CO)_2W(Si(H)_2C{\equiv}CH)$ (**9**), in which the C≡C triple bond coordinates with the W center, as shown in Figure 6. The C≡C triple bond gradually approaches the W center in the reaction. Consistent with this geometry change, one of the π-orbitals of the C≡C triple bond becomes considerably lower in energy (see Figure S3, Supporting Information). The approach of the C≡C triple bond to the W center induces a change in the direction of the sp^3-orbital on Si which interacts substantially with the W center in **8**, to increase the sp^3-orbital

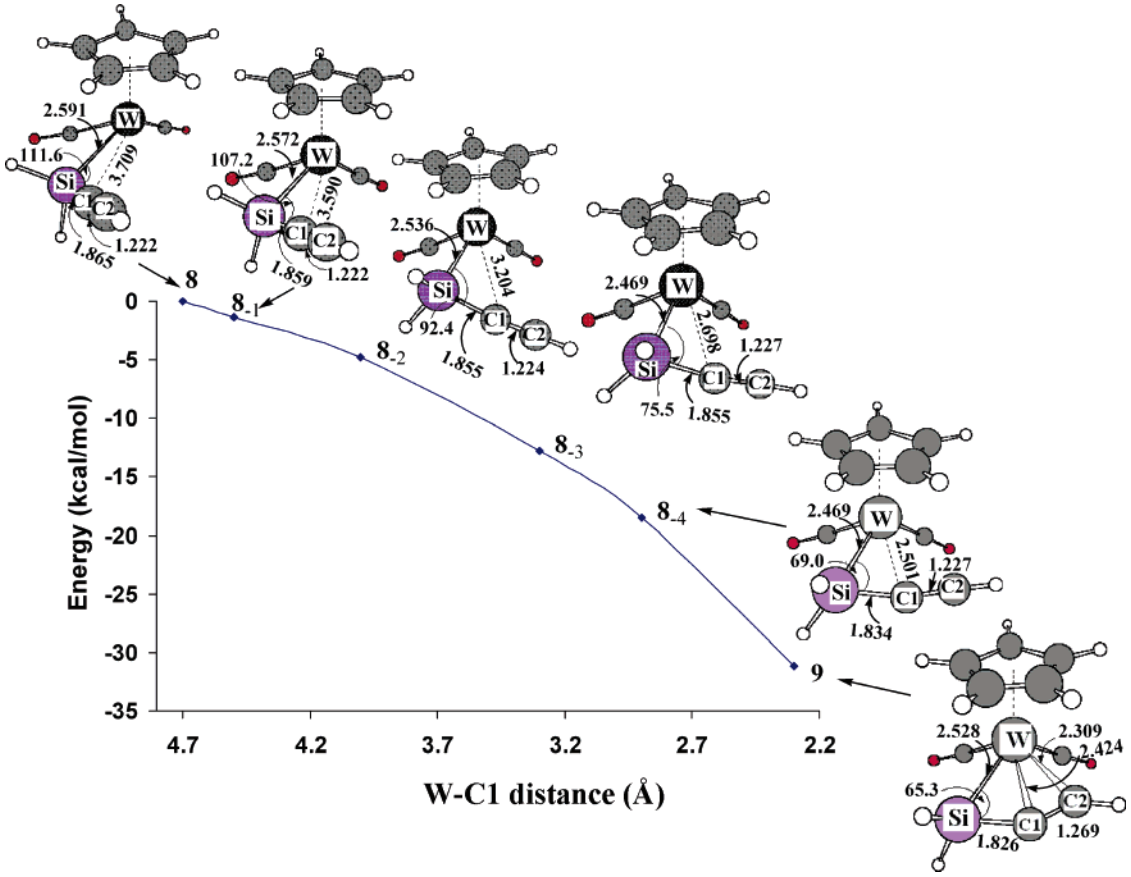

Figure 6. Geometry[a] and energy[b] changes resulting from the conversion of $Cp(CO)_2W(Si(H)_2C{\equiv}CH)$ (**8**) to $Cp(CO)_2W(Si(H)_2C{\equiv}CH)$ (**9**). [a]DFT/BS-I optimization was carried out. Bond lengths are in angstroms, and bond angles are in degrees. [b]DFT/BS-II calculation (in kcal/mol).

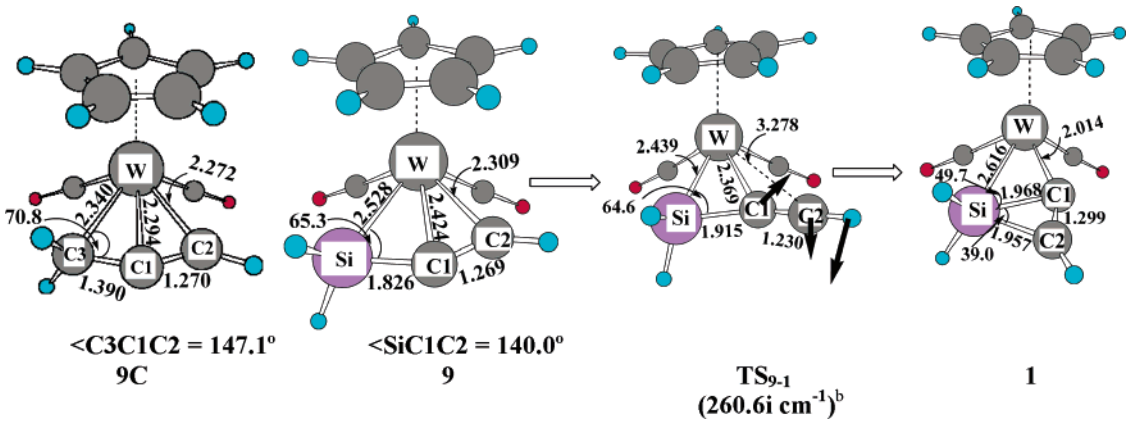

Figure 7. Geometry[a] of $Cp(CO)_2W(C(H)_2C{\equiv}CH)$ (**9C**) and geometry changes[a] resulting from the conversion of $Cp(CO)_2W(Si(H)_2C{\equiv}CH)$ (**9**) to $Cp(CO)_2W(C{\equiv}CH)(SiH_2)$ (**1**). [a]DFT/BS-I optimization was carried out. Bond lengths are in angstroms, and bond angles are in degrees. [b]Arrows in $\mathbf{TS_{9-1}}$ represent important movement of atoms in imaginary frequency. Imaginary frequency is given in parentheses. DFT/BS-I calculation.

energy. However, the energy does not increase much because this sp^3-orbital changes to the HOMO of a silapropargyl-type $Si(H)_2C{\equiv}CH$ species, which will be discussed below in detail. As a result, the conversion of **8** to **9** takes place easily, with no barrier and considerably large exothermicity, as shown in Table 3. The DFT-calculated exothermicity (31.2 kcal/mol) is similar to the MP4(SDQ)-calculated value (34.5 kcal/mol) but somewhat smaller than the MP4(SDTQ)-calculated value (43.3 kcal/mol), suggesting that the exothermicity is between 31 and 43 kcal/mol. Thus, it can be considered that this process is considerably exothermic.

Geometry and Bonding Nature of $Cp(CO)_2W(Si(H)_2C{\equiv}CH)$ (9). Here, we wish to discuss the bonding nature of **9** because this species is of considerable interest. It is considered to be the Si analogue of a transition metal−propargyl complex, and such a species has not been reported yet. To clarify the characteristic features of **9**, we optimized the model propargyl complex, $Cp(CO)_2W(C(H)_2C{\equiv}CH)$ (**9C**). As shown in Figure 7, the C1−C2 distance of **9** is almost the same as that of **9C**. The Si−C1 (1.826 Å) and C1−C2 (1.269 Å) bond distances of **9** are intermediate between the Si−C single and the Si═C

double bonds and between C=C double and C≡C triple bonds, respectively; R(Si−C) = 1.895 and 1.717 Å in H_3Si-CH_3 and $H_2Si=CH_2$, respectively, and R(C−C) = 1.334 and 1.209 Å in $H_2C=CH_2$ and HC≡CH, respectively, where the DFT/BS-I-optimized values are presented. The Si−C1−C2 angle of the $[Si(H)_2CCH]^-$ ligand in **9** is 140°, which is similar to that of **9C**. All these geometrical features suggest that the $[SiH_2CCH]^-$ ligand in **9** can be considered as a silicon analogue of the η^3-propargyl/allenyl group. Of course, some differences between **9** and **9C** are observed. For instance, the W−C2 distance is somewhat longer in **9** than in **9C**, while the W−C1 distance of **9** is much longer than that of **9C**. These results are not surprising. Because Si is larger than C, the W−Si distance of **9** is longer than the W−C3 distance of **9C**, which leads to the longer W−C1 and W−C2 distances in **9** than in **9C**.

To investigate the coordinate bond of the $[Si(H)_2CCH]^-$ ligand, we examined several important molecular orbitals of **9** and **9C**, as shown in Figure 8A,B. The HOMO and HOMO-1 of **9** mainly consist of a d-orbital, similar to the HOMO and HOMO-1 of **1**. The remaining three d-orbitals are in unoccupied molecular orbitals in both complexes. These results are consistent with the fact that the W center takes a 2+ oxidation state in **9** and **9C**. There are two important molecular orbitals for the interaction: HOMO-2 and HOMO-6. Because these orbitals involve the bonding interaction between the $Si(H)_2CCH$ moiety and W, we first discuss frontier orbitals of $^\bullet Si(H)_2CCH$ and the usual propargyl groups. The HOMO of both $^\bullet Si(H)_2CCH$ and $^\bullet C(H)_2CCH$ is a nonbonding π-orbital ($\varphi_{n\pi}$) which consists of p-orbitals of terminal C and Si (or C) atoms, as shown in Figure 8C,D. Although the two p-orbitals of the terminal C atoms contribute to the HOMO to almost the same extent in $^\bullet C(H)_2CCH$, the p-orbital of Si contributes more to the HOMO than that of C in $^\bullet Si(H)_2CCH$. This is because the p-orbital of Si is at higher energy than that of C; for instance, the p-orbital of $^\bullet SiH_3$ is at −5.39 eV, and that of $^\bullet CH_3$ is at −6.41 eV, where orbital energies calculated with the DFT/BS-II method are presented (Hartree−Fock orbital calculation provides a similar energy difference between them).[49] The HOMO-2 is, however, considerably different between $^\bullet C(H)_2CCH$ and $^\bullet Si(H)_2CCH$; it is the usual π-orbital in $^\bullet C(H)_2CCH$, which is similar to the π-orbital of π-allyl group. In $^\bullet Si(H)_2CCH$, on the other hand, it is similar to the π-orbital of the C=C double bond to which the p-orbital of Si moderately contributes. The shape of the HOMO is easily understood in terms of allyl-type orbital mixing, as follows: The p-orbital of Si overlaps with the π-orbital of acetylide in an antibonding way, as shown in Scheme 5A, because the p-orbital is at higher energy than the π-orbital. The π^*-orbital of acetylide mixes into this orbital in a bonding way with the p-orbital of Si, to weaken the antibonding overlap between the p-orbital of Si and the π-orbital. This mixing significantly decreases the contribution of the C1 p-orbital and increases very much that of the C2 p-orbital to afford $\varphi_{n\pi}$. This $\varphi_{n\pi}$-orbital overlaps with the empty d-orbital of W in a bonding way to form the HOMO-2 of **9**. In $^\bullet C(H)_2CCH$, the p-orbitals of three C atoms overlap with each other in a bonding way, to form the HOMO-2 (φ_π), as shown in Scheme 5B. Thus, the φ_π-orbital delocalizes to the terminal C atom. This φ_π-orbital overlaps with the acceptor orbital of W in a bonding way to afford the HOMO-6, as shown in Figure 8B. The different shape of the HOMO-2 of $^\bullet Si(H)_2CCH$ is interpreted in terms of the higher energy of the Si p-orbital. Because the p-orbital of Si is at much higher energy than that of C, as described above, the former orbital contributes much less to the HOMO-6 than the latter orbital, as shown in Scheme 5C. As a result, the φ_π-orbital moderately delocalizes onto the Si atom, as shown in Figure 8C. Because of the rather localized φ_π-orbital of $^\bullet Si(H)_2CCH$, the HOMO-6 of **9** is considerably different from that of **9C**, as shown in Figure 8A,B.

From all these results, it should be concluded that, although **9** is considered to be the Si analogue of a propargyl/allenyl complex and the nonbonding π-orbital is similar to that of the propargyl/allenyl group, the conjugation between Si and C atoms

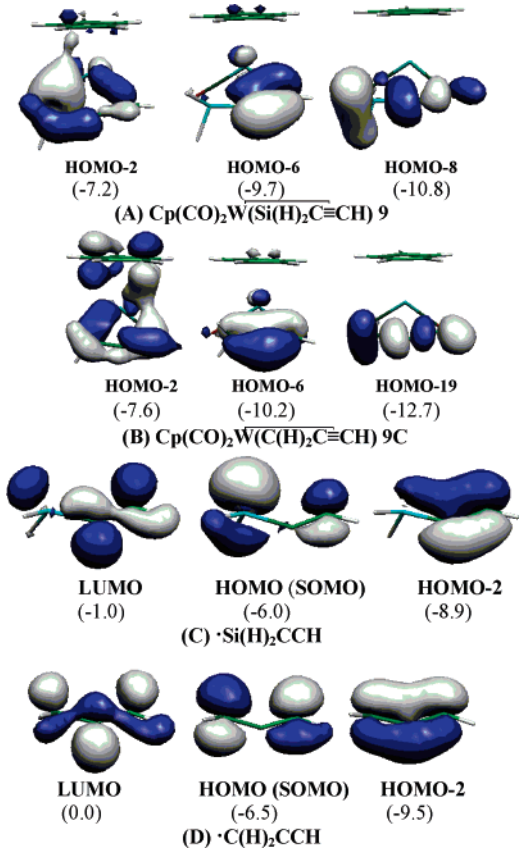

Figure 8. Several important Kohn−Sham orbitals observed in $Cp(CO)_2W(Si(H)_2C\equiv CH)$ (**9**), $Cp(CO)_2W(C(H)_2C\equiv CH)$ (**9C**), and their fragments, $^\bullet Si(H)_2CCH$ and $^\bullet C(H)_2CCH$. In parentheses are orbital energies (in eV).

Scheme 5

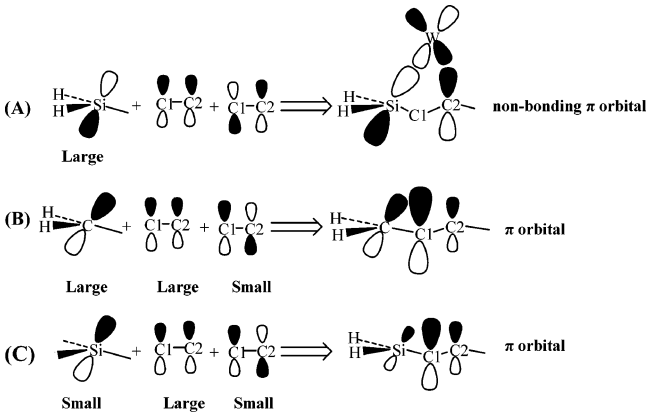

(49) The HF-calculated p-orbital of $^\bullet SiH_3$ is at −7.85 eV and that of $^\bullet CH_3$ is at −10.47 eV.

Table 4. Activation Barrier (E_a)[a] and Reaction Energy (ΔE)[a] in the Conversion of $Cp(CO)_2W(Si(R^2)_2C{\equiv}CH)$ (**9**) to $Cp(CO)_2W(C{\equiv}CH)(SiH_2)$ (**1**)

method	E_a (kcal/mol)	ΔE (kcal/mol)
DFT	15.3	−4.9
MP2	20.7	0.4
MP3	14.0	−1.4
MP4(DQ)	15.5	−0.1
MP4(SDQ)	14.8	−0.9
MP4(SDTQ)	18.8	−0.6
CCSD(T)	15.8	−0.7

[a] E_a is the energy difference between transition state and reactant, and ΔE is the energy difference between product and reactant. BS-II was employed.

is very weak in the π-orbital, unlike the π-orbital of the usual propargyl/allenyl group, in which considerable conjugation is clearly observed.

Conversion of $Cp(CO)_2W(Si(H)_2C{\equiv}CH)$ (9) to $Cp(CO)_2W(C{\equiv}CH)(SiH_2)$ (1). Because **Form-A** is the correct representation of $Cp(CO)_2W(SiH_2)(C{\equiv}CH)$ (**1**), as discussed above, the conversion of **9** to **1** involves α-Si−C σ-bond activation via the interesting 1,2-alkynyl shift, which takes place through the transition state $\mathbf{TS_{9-1}}$, as shown in Figure 7. In the imaginary frequency of $\mathbf{TS_{9-1}}$, the direction of the sp-orbital of the C≡C−H group is changing toward the W center. As a result, the W−C1 distance shortens to 2.369 Å and the W−C2 distance lengthens considerably to 3.278 Å in $\mathbf{TS_{9-1}}$. At the same time, the Si−C1 distance lengthens to 1.915 Å in $\mathbf{TS_{9-1}}$, while it is still shorter than that in **1** by 0.053 Å. All these results indicate that the Si−C1 σ-bond and the W−C2 bond of **9** are going to be broken and the W−C1 bond is going to be formed in $\mathbf{TS_{9-1}}$. Interestingly, the W−Si distance of $\mathbf{TS_{9-1}}$ is shorter than those of **9** and **1** by 0.089 and 0.177 Å, respectively. The C1−C2 distance of $\mathbf{TS_{9-1}}$ is shorter than those of **9** and **1**, too. These interesting geometry changes relate to the interaction between $[Si(H)_2CCH]^-$ and the W center, which will be discussed below.

This conversion reaction takes place easily with a moderate activation barrier of 15.3 (15.8) kcal/mol and a small exothermicity of 4.9 (0.7) kcal/mol, as shown in Table 4, where the DFT- and CCSD(T)-calculated energies are given without and in parentheses, respectively. The CCSD(T) and DFT methods present a similar activation barrier, but the MP4(SDTQ) method presents a moderately larger value. On the other hand, the DFT-calculated exothermicity is moderately larger than the others. It is likely that the DFT- and CCSD(T)-calculated activation barriers and the MP4(SDTQ)- and CCSD(T)-calculated exothermicities are reliable.

The d-orbital population of W changes little upon going to **1** (5.77e) from **9** (5.77e), but it is moderately larger in $\mathbf{TS_{9-1}}$ (5.85e) than in **9** and **1**, where the DFT/BS-II-calculated values are given in parentheses. We found above that W has a 2+ oxidation state in both **9** and **1**. This is consistent with the d-orbital populations being almost the same in **9** and **1**. These results indicate that the conversion from **9** to **1** takes place without changing the oxidation state of W. The moderate increase in W d-orbital population in $\mathbf{TS_{9-1}}$ relates to the interactions in the transition state, as will be discussed below.

It is of considerable interest to clarify the reason why the α-Si−C σ-bond activation takes place easily with a moderate activation barrier. To clearly understand this α-Si−C σ-bond activation, we carried out an intrinsic reaction coordinate (IRC) calculation and examined the molecular orbitals along the reaction coordinate, as shown in Figure 9, where energies of three important orbitals are plotted against the reaction coordinate (see Figure 9B). One is HOMO-8, which mainly consists of the Si−C1 bonding orbital in **9**. This orbital energy does not change very much in the reaction, although the Si−C bond is broken. This is because the sp lone-pair orbital of acetylide decreases the bonding overlap with the sp^3-orbital of the silyl group by changing its orientation from the Si atom toward the W center, but it starts to overlap with the acceptor orbital of W, as shown in Scheme 6. On the other hand, the HOMO-6 increases considerably in energy upon going to $\mathbf{9_{-5}}$ from **9** and then becomes considerably lower in energy upon going to **1** from $\mathbf{9_{-5}}$ (see Figure 9 for $\mathbf{9_{-1}}$ to $\mathbf{9_{-8}}$). These changes are easily understood in terms of the interaction of the acetylide π-orbital with either the acceptor orbital of W or the empty p-orbital of the silylene. The HOMO-6 of **9** mainly consists of the bonding interaction between the π-orbital of acetylide and the acceptor orbital of W, as shown in Figure 8A. Because the acetylide moiety changes its orientation upon going to $\mathbf{TS_{9-1}}$ from **9**, the bonding overlap between the acetylide π-orbital and the acceptor orbital of W decreases, as shown in Figure 9, which increases the HOMO-6 energy. However, the acetylide π-orbital starts to overlap with the empty p-orbital of silylene upon going to **1** from $\mathbf{9_{-5}}$, to stabilize the HOMO-6 in energy.

Scheme 6

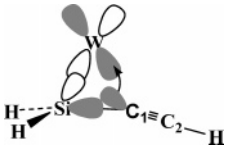

The HOMO-2 energy changes in a complicated manner: it first increases and reaches the maximum before $\mathbf{TS_{9-1}}$. It then decreases upon going to $\mathbf{9_{-5}}$ from $\mathbf{9_{-3}}$. At $\mathbf{TS_{9-1}}$, it is decreasing. After $\mathbf{9_{-5}}$, it changes little. The HOMO-2 of **9** mainly consists of the bonding overlap between the empty d-orbital of W and the $\varphi_{n\pi}$-orbital, as shown in Figure 8A. The energy increase in the early stage of the reaction is easily understood in terms of the bonding overlap between the p-orbital of C2 and the empty d-orbital of W becoming small upon going to $\mathbf{9_{-3}}$ from **9**, as clearly observed in Figure 9. Upon going from $\mathbf{9_{-3}}$ to $\mathbf{9_{-5}}$ through $\mathbf{TS_{9-1}}$, silylene is gradually formed. Its lone-pair orbital overlaps with the W center in a bonding way around $\mathbf{TS_{9-1}}$, which lowers the HOMO-2 in energy, as shown in Figure 9. This is consistent with the shorter W−Si distance and the larger W d-orbital population at $\mathbf{TS_{9-1}}$ compared to those in **9** and **1**. In the latter half of this reaction from $\mathbf{9_{-5}}$ to **1**, silylene changes its direction toward the C1 atom, which decreases the overlap between the lone-pair orbital and the acceptor orbital of W, increasing the energy of HOMO-2. However, the π*-orbital of acetylide starts to overlap with the lone-pair orbital of silylene in a bonding way upon going to **1** from $\mathbf{9_{-5}}$, which decreases the HOMO-2 energy. Because these two effects compensate each other, the HOMO-2 energy changes little in the latter half of the reaction.

From these results, three important conclusions are extracted: (1) The origin of the activation barrier is the weakening of the bonding interaction between the $\varphi_{n\pi}$-orbital of the silapropargyl group and the acceptor orbital of W. (2) The

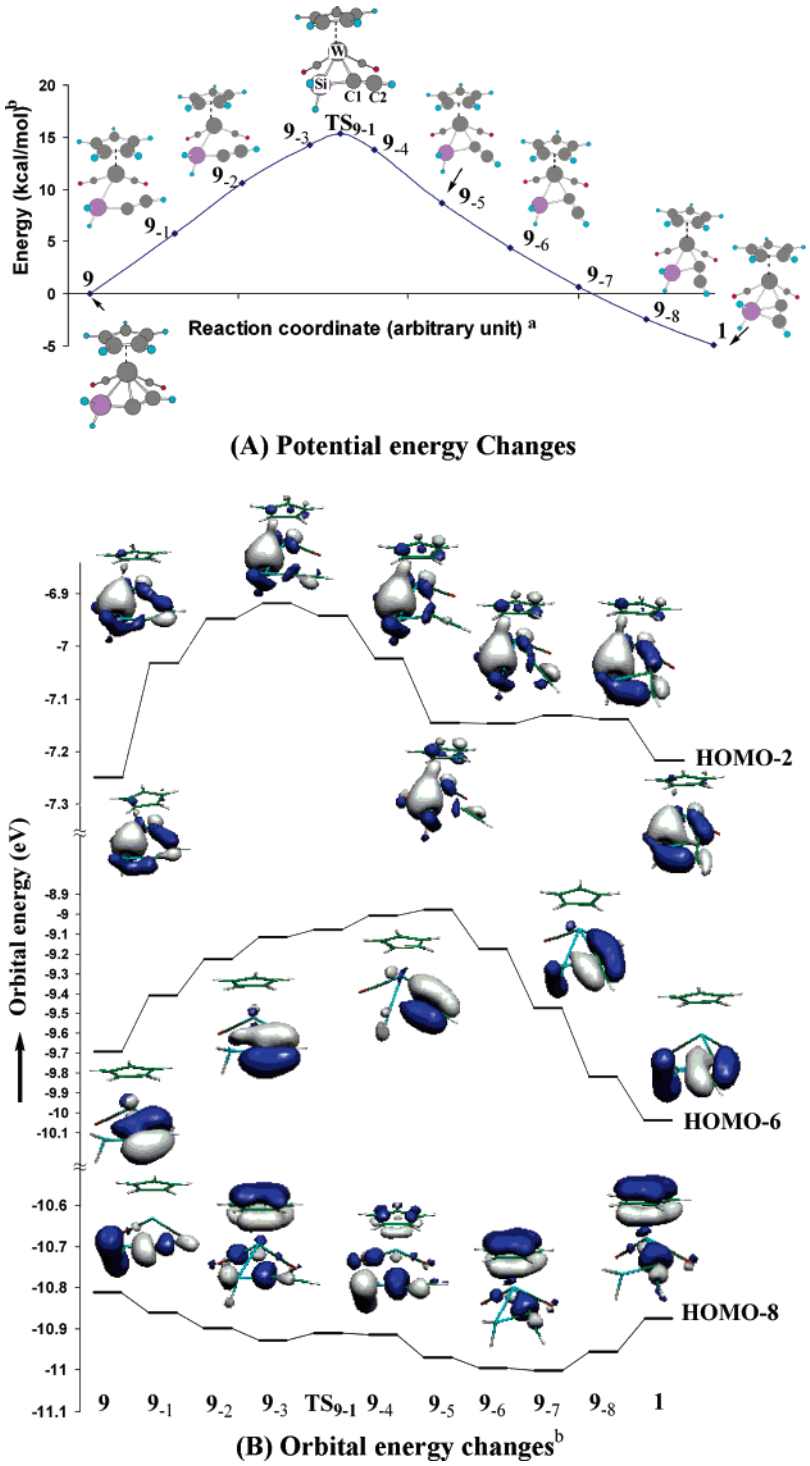

Figure 9. Changes in potential energy and orbital energies resulting from the conversion of $Cp(CO)_2W(\overline{Si(H)_2C{\equiv}CH})$ (**9**) to $Cp(CO)_2W(C{\equiv}CH)(SiH_2)$ (**1**). See Figure 7 for **9**, $\mathbf{TS}_{9-1}$, and **1**. [a]Reaction coordinates from IRC calculation with the DFT/BS-I method. [b]DFT/BS-II calculation. In Hartree−Fock orbitals, essentially the same energy changes are observed (see Supporting Information, Figure S4).

π-orbital of acetylide is stabilized in energy by the interaction with the empty p-orbital of silylene. (3) The lone pair of silylene is stabilized in energy by the interaction with the π^*-orbital of acetylide. In other words, the driving force for the 1,2-alkynyl shift is the CT interactions between the π-orbital of acetylide and the empty p-orbital of silylene and between the lone-pair orbital of silylene and the π^*-orbital of acetylide.

Conclusions

The geometry and bonding nature of $Cp^*(CO)_2W(C{\equiv}C^tBu)(SiPh_2)$ and all the steps of the reaction leading to its formation from $Cp^*(CO)_2W(Me)(HSi(Ph)_2C{\equiv}C^tBu)$ were theoretically investigated with DFT, MP2 to MP4(SDTQ), and CCSD(T) methods, where $Cp(CO)_2W(C{\equiv}CH)(SiH_2)$ (**1**) and $Cp(CO)_2W(Me)(Si(H)_3C{\equiv}CH)$ (**5**) were adopted as their models, respec-

tively. The geometrical features and the bonding nature indicate that **1** is neither a pure silacyclopropenyl complex of W nor a pure silylene acetylide complex of W. Although no pure silacyclopropenyl group is formed in **1**, the orbitals of **1** resemble well those observed in the formation of silacyclopropene from silylene and acetylene. Those orbitals are formed through interactions of the π- and π*-orbitals of acetylide with the lone pair and empty p-orbitals of silylene. In **1**, CT occurs from the π-orbital of the acetylide moiety to the empty p-orbital of silylene, and simultaneously the other CT occurs from the sp^2 lone-pair orbital of silylene to the π*-orbital of acetylide. From these frontier orbitals, as well as the geometry of **1**, it can be concluded that the $CCH(SiH_2)$ moiety of **1** is an intermediate species trapped by the W center in the formation of silacyclopropene from silylene and acetylene. The substituent on the acetylide group considerably influences the geometry of **1**.

Complex **1** is formed from **5** through several steps, as follows: $Cp(CO)_2W(Me)(Si(H)_3C{\equiv}CH)$ (**5**) first converts to $Cp(CO)_2W(H)(Me)(Si(H)_2C{\equiv}CH)$ (**6**) with no barrier and considerable exothermicity through Si−H oxidative addition. Then, **6** converts to $Cp(CO)_2W(CH_4)(Si(H)_2C{\equiv}CH)$ (**7**) through the reductive elimination of methane, with a moderate activation barrier of 10.7 (11.8) kcal/mol, where the DFT- and MP4(SDTQ)-calculated energies are given without parentheses and in parentheses, respectively. This reductive elimination is almost thermoneutral. After methane dissociation from **7**, coordination of the C≡C triple bond to W takes place with no barrier and a large exothermicity of 31.2 (43.3) kcal/mol, to afford $Cp(CO)_2W(\overline{Si(H)_2C{\equiv}CH})$ (**9**). Finally, **9** converts to $Cp(CO)_2W(C{\equiv}CH)(SiH_2)$ (**1**) through α-Si−C σ-bond activation with moderate activation barriers of 15.3, 18.8, and 15.8 kcal/mol and exothermicities of 4.9, 0.6, and 0.7 kcal/mol, which are calculated with the DFT, MP4(SDTQ), and CCSD(T) methods, respectively. This moderate activation barrier arises from the stabilization of the π-orbital of acetylide by the bonding interaction with the empty p-orbital of silylene and that of the lone pair of silylene by the bonding interaction with the π*-orbital of acetylide. In other words, α-Si−C σ-bond activation easily occurs via a 1,2-alkynyl shift because of these bonding interactions.

Complex **9** is a silicon analogue of the η^3-propargyl/allenyl complex of W, but the delocalization in $[H_2SiCCH]^-$ is much less than that in $[H_2CCCH]^-$. The nonbonding π-orbital of the H_2SiCCH moiety is essentially the same as that of the propargyl group, but the π-conjugation between Si and C atoms is very weak, unlike the sufficient π-conjugation in the propargyl complex. Thus, **9** is understood in terms of 50% of the Si analogue of a tungsten−η^3-propargyl complex and 50% of a tungsten−alkynylsilyl complex.

Acknowledgment. This work was financially supported by Grants-in-Aid on basic research (No. 1835005), Priority Areas for "Molecular Theory" (No. 461), Creative Scientific Research, and NAREGI project from the Ministry of Education, Science, Sports, and Culture. Some of the theoretical calculations were performed with SGI workstations at the Institute for Molecular Science, Okazaki, Japan.

Supporting Information Available: Complete ref 41; geometries of $HCCR^1$ (R^1 = H, Me, or ^{t}Bu); several important Kohn−Sham orbitals observed in the conversion of **5** to **7** and discussions; changes of orbital energy in the conversion of **8** to **9**; changes of Hartree−Fock orbital energy in the conversion of **9** to **1**; effects of functional and basis set on the structural parameters of **1**; and Cartesian coordinates and total energies of important species, including transition states. This material is available free of charge via the Internet at http://pubs.acs.org.

JA0625374